Nanospheres-Incorporated Implantable Hydrogel as a Trans-Tissue Drug Delivery System

Dan Ding,[†] Zhenshu Zhu,[†] Rutian Li,[§] Xiaolin Li,[§] Wei Wu,[†] Xiqun Jiang,[†,*] and Baorui Liu[§]

[†]Laboratory of Mesoscopic Chemistry and Department of Polymer Science & Engineering, College of Chemistry & Chemical Engineering, Nanjing University, Nanjing, People's Republic of China, and [§]Comprehensive Cancer Center of Drum-Tower Hospital, Medical School of Nanjing University & Clinical Cancer Institute of Nanjing University, Nanjing, People's Republic of China

ABSTRACT The objective of this study is to investigate the anticancer efficacy of a drug delivery system comprised of gelatin hydrogel (jelly) containing cisplatin (CDDP)-loaded gelatin/poly(acrylic acid) nanoparticles by peritumoral implantation and to compare the treatment response between the implantation administration of the jelly and intravenous (i.v.) administration of the nanoparticles. It is found that the implantation of the jelly containing CDDP-loaded nanoparticles on tumor tissue exhibited significantly superior efficacy in impeding tumor growth and prolonging the lifetime of mice than that of i.v. injection of CDDP-loaded nanoparticles in a murine hepatoma H_{22} cancer model. An *in vivo* biodistribution assay performed on tumor-bearing mice demonstrated that the jelly implant caused much higher concentration and retention of CDDP in tumor and lower CDDP accumulation in nontarget organs than that of i.v. injected nanoparticles. Immunohistochemical analysis demonstrated that the nanoparticles from the jelly can be distributed in tumor tissue not only by their diffusion but also by the vasculature in the implantation region into tumor interior, enabling CDDP to efficiently reach more viable cells of tumor compared with i.v. injected nanoparticles. Thus, nanoparticles for peritumoral chemotherapy are promising for higher treatment efficacy due to increased tumor-to-normal organ drug uptake ratios and improved drug penetration in tumors.

KEYWORDS: polymer nanoparticles · polymer hydrogel · drug delivery · peritumoral chemotherapy · antitumor effect

The treatment of solid tumors can be improved by virtue of nanoparticulate formulation to deliver antitumor agents in passive and active targeting fashions.[1−4] To reach cancer cells in a tumor, a blood-borne therapeutic particle must enter the tumor vasculature, cross the vessel wall, and transport through the interstitial compartment.[5] However, the limited blood supply in tumors,[6] detention by other tissues during the journey,[7] and insufficient penetration in tumor tissue[8−10] make it hard for nanoparticles to deliver an optimal dose of agent to cancer cells, which greatly limits their anticancer effect. In experimental tumor models, intratumoral administration of drug-loaded nanoparticles has been found to be an alterative method for cancer treatment in addition to limiting systemic exposure.[11] Unfortunately, the weak ability to efficiently penetrate the tumor and affect cells distant from the injection site also limits the therapeutic efficacy of nanoparticles.[12,13] Moreover, after debulking surgery as the initial primary treatment for major ovarian or gastrointestinal cancers, the residual tumors peritoneally disseminated can hardly be observed, and it is difficult to inject a nanoparticle solution into so many small metastatic tumors.[14,15] In addition, it has also been demonstrated that the diffusion of the loaded drug is greatly improved by peritumoral administration as contrasted with intratumoral injection, leading to much better antitumor effect.[16] In parallel, biocompatible, biodegradable, and drug-releasing polymeric implants, such as polymeric hydrogels,[14,15,17,18] injectable thermosensitive hydrogel,[19] injectable microspheres,[16] and polymer millirods,[20] have shown certain prolonged tumor drug exposure and sustained drug release as well as reduced systemic toxicity. Furthermore, the drug controlled releasing polymer hydrogel can be used to coat the tumor and any suspicious site of tumor to give rise to high drug concentration in location.[14] Although there are several advantages to such systems, they also suffer from rapid drug clearance in tumor, poor drug penetration in tumor tissues as well as cell membranes, and drug dosage limited by implant shape and surface area. Therefore, more efficient treatment of solid tumors is highly desirable to further improve the concentration and penetration of drug in tumor tissues and cells and reduce systemic toxicity.

As a trial, our strategy is to design a trans-tissue drug delivery system for peritumoral chemotherapy. We incorporated cisplatin (CDDP)-loaded gelatin (GEL)/poly(acrylic acid)

* Address correspondence to jiangx@nju.edu.cn.

Received for review August 24, 2010 and accepted March 23, 2011.

Published online March 23, 2011
10.1021/nn102138u

(PAA) nanoparticles into the physically cross-linked gelatin hydrogel to obtain a nanoparticle-encapsulated matrix, which can be implanted and plastered on the tumor mass in any shape. Gelatin is a biocompatible, biodegradable, and nontoxic material that has a long history of safe use in medical and pharmaceutical applications.[15] Type-B gelatin, with an isoelectric point of 4.7−5.2, possesses a large number of pendant functional groups such as amine groups and carboxylic groups.[21] The GEL-PAA nanoparticles, which were well-dispersed and stable in aqueous solution, were first prepared using a polymer−monomer pair reaction system.[21,22] Then, CDDP, a well-known anticancer agent,[23] was incorporated into the prepared GEL-PAA nanoparticles by the complexation between the platinum of CDDP and the carboxylic group of PAA and gelatin of nanoparticles. Finally, the obtained CDDP-loaded GEL-PAA nanoparticles were encapsulated into the physically cross-linked gelatin hydrogel. This system, which we called CDDP-loaded GEL-PAA nanoparticles-encapsulated jelly (CDDP-NP-Jelly), is of particular interest and importance. First, the jelly is able to gradually transfer into a viscous sol above 37 °C, which acts as a reservoir to provide the CDDP-loaded GEL-PAA nanoparticles locally to the tumor and offers continuous release of CDDP over a prolonged period of time. Second, implanting or plastering the jelly onto a tumor mass increases the contact areas between nanoparticles and tumor tissue, which may permit the nanoparticles to diffuse into the tumor tissue from many more sites, greatly improving the spatial distribution of the nanoparticles within the tumor, in contrast to limited spatial diffusion of nanoparticles from only one injection site by intratumoral administration. Third, since the tumor periphery region is the most vascularized region,[24] implanting or plastering the jelly at the peritumoral sites may favor the diffusion of CDDP-loaded nanoparticles into the nearby blood vessels, directly delivering drug along blood flow into the other portions of the tumor, especially the inner part of the tumor. On the basis of these reasons, in the present work, we examined the anticancer efficacy, drug pharmacokinetics, and biodistribution over time resulting from implantation of jelly onto the surface of H_{22} tumor xenografts for comparison with the same amount of CDDP-loaded GEL-PAA nanoparticles administered as intravenous (i.v.) injection. Additionally, the penetration of GEL-PAA nanoparticles in tumor tissue was also examined by immunohistochemical analysis.

RESULTS

Synthesis and Characterization of CDDP-Loaded GEL-PAA Nanoparticles. In this study, the GEL-PAA nanoparticles were prepared by dissolving GEL into acrylic acid (AA) aqueous solution, followed by polymerization of AA initiated by $K_2S_2O_8$. To investigate the changes in the complex particles during the polymerization process, the size and zeta potential as a function of the polymerization time were estimated by dynamic light scattering (DLS). As shown in Figure 1A, the average hydrodynamic diameter of the sample is around 700 nm and the zeta potential is 26.8 mV before the initiation by $K_2S_2O_8$, suggesting that the GEL and AA monomers are most likely to form loose aggregates before the polymerization. At this stage, the pH value of the solution was measured to be 4.2. After 30 min of polymerization of AA, the solution changed from clear to opalescent and the size and zeta potential of the aggregates become 244 nm and 21.6 mV, respectively. Then the size of aggregates slowly contracted to about 110 nm and the zeta potential decreases to around 20 mV after 150 min of polymerization. The pH value of the system went from 4.2 before the reaction down to about 3.3 at the end of the polymerization due to the decomposition of $K_2S_2O_8$, causing a decrease in pH value of the system.[25] In addition, it is also found that the molecular weight of PAA in GEL-PAA aggregates increases with polymerization time, which is about 2300 Da at the end of the polymerization (Figure 1B).

On the basis of these results, a possible formation mechanism of the GEL-PAA nanoparticles is proposed as illustrated in Scheme 1. Before the polymerization, anionic AA monomers and cationic GEL chains form loose aggregates in the solution with a pH value of around 4.2 (isoelectric point = 4.7−5.2 for GEL and pK_a = 4.25 for AA[22]), and the GEL-AA aggregates are stabilized by the GEL chains that are positively charged. Upon polymerization of AA, anionic PAA generates and electrostatically interacts with GEL chains to form loose interpolyelectrolyte complex nanoparticles. As the polymerization proceeds, the electrostatic interaction between GEL and PAA becomes stronger with the increase of the molecular weight of PAA, resulting in a tendency toward particle shrinkage and a decrease in the particle size. Moreover, the zeta potential of the GEL-PAA particles stays positive during the whole polymerization, with the pH value changing from 4.2 to 3.3, suggesting that the GEL-PAA nanoparticles are stabilized by an outer layer of GEL with protonated amine groups.

To further enhance the stability of GEL-PAA nanoparticles for drug delivery application, we used a cross-linker, 2,2′-(ethylenedioxy)bis(ethylamine), to chemically cross-link the carboxylic groups in the nanoparticles. To study the effect of the amount of cross-linker on nanoparticle size, various cross-linker amounts were introduced into the system with the molar ratio of amine groups in the cross-linker to carboxylic groups in the system in the range of 0:1 to 1:1 (Table 1). It is found that the size of the nanoparticles in phosphate-buffered saline (PBS) solution (pH 7.4) decreases with increasing the amount of cross-linker, and the sizes of cross-linked nanoparticles with different cross-linking

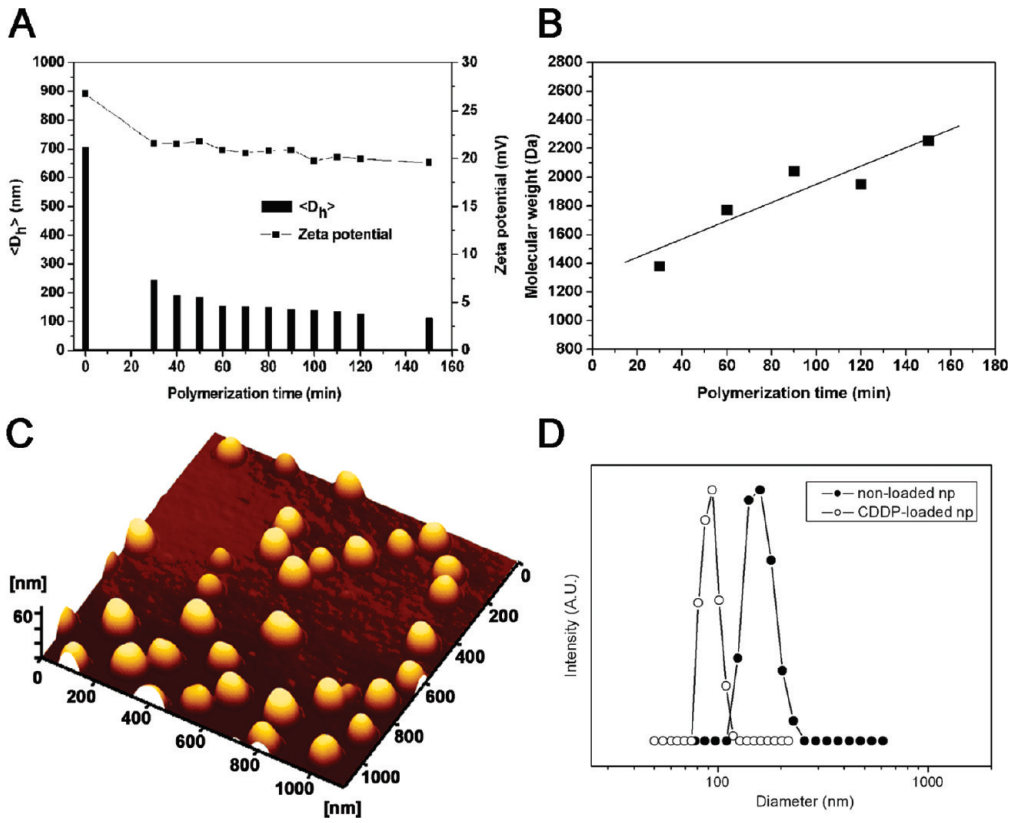

Figure 1. (A) GEL-PAA particle size and zeta potential at different polymerization times. (B) Molecular weight of PAA in GEL-PAA nanoparticles as a function of polymerization time. (C) AFM image of cross-linked GEL-PAA nanoparticles. (D) Hydrodynamic diameter distribution of empty and CDDP-loaded GEL-PAA nanoparticles at 37 °C by DLS.

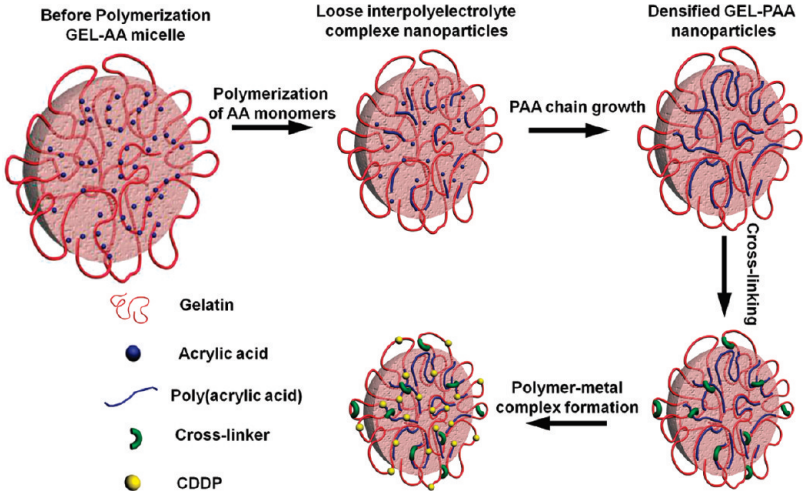

Scheme 1. Schematic illustration of the synthesis of CDDP-loaded GEL-PAA nanoparticles.

density are all less than 200 nm compared with that of un-cross-linked ones (422 nm) in PBS solution. Furthermore, since the isoelectric point of type-B gelatin used in this study is 4.7−5.2, GEL molecules are negatively charged with ionized carboxylic groups at pH 7.4, resulting in negative zeta potential values of the GEL-PAA nanoparticles before and after cross-linking. For the next encapsulation of CDDP, cross-linked GEL-PAA nanoparticles at a molar ratio of 0.5:1 for amine groups of the cross-linker and carboxylic groups in the system were selected because they show satisfactory size (160 nm) and stability in PBS (their size hardly changed for at least two weeks) as well as have enough carboxylic groups to load CDDP. The morphology of the cross-linked GEL-PAA nanoparticles (0.5:1) was examined by atomic force microscopy (AFM) and transmission electron microscopy (TEM), respectively (Figure 1C and Figure S1 in the Supporting Information).

TABLE 1. Effect of Amount of Cross-Linker on Nanoparticle Size and Zeta Potential in PBS Solution (pH 7.4)

$[NH_2]$:[COOH][a]	diameter ± SD (nm)	polydispersity	zeta potential ± SD (mV)
0	422 ± 9	0.23	−37.0 ± 4.8
0.25:1	186 ± 5	0.14	−29.3 ± 3.6
0.5:1	160 ± 5	0.13	−23.5 ± 4.0
1:1	149 ± 3	0.13	−20.1 ± 3.2

[a] Ratio of amino groups from 2,2′-(ethylenedioxy)bis(ethylamine) to the carboxylic groups from GEL-PAA nanoparticles.

Both images give the appearance of the particles, clearly showing that all nanoparticles are well dispersed and in spherical shape with a uniform size of about 110 nm, which is a little smaller than that observed by DLS due to shrinking in the dry state.

Next, CDDP was loaded into the nanoparticles through the interaction between the platinum of CDDP and the carboxylic group of the nanoparticles (Scheme 1).[26] A satisfactory CDDP loading content (17%) as well as high encapsulation efficiency (85%) was achieved. The size and size distribution of nanoparticles before and after encapsulating CDDP were examined by DLS (Figure 1D). It can be seen that the mean diameter of drug-loaded particles (93.3 nm) is smaller than that of the nonloaded ones (160.3 nm), suggesting the formation of a polymer−metal complex in the nanoparticles, as we expect. In addition, CDDP-loaded GEL-PAA nanoparticles showed higher stability than the empty ones, and their size hardly changed even after 30 days in PBS solution.

Preparation and Characterization of CDDP-NP-Jelly. For the purpose of peritumoral chemotherapy using CDDP-loaded GEL-PAA nanoparticles, we utilized physically cross-linked gelatin hydrogel as the carrier of the nanoparticles that are able to be surgically plastered on the tumor tissue. Gelatin, made from collagen through a hydrolysis process, can dissolve in water above its melting temperature (about 35 °C) and lead to gelation upon cooling below the melting temperature by gelatin molecules partially reverting to ordered triple helical conformation, which becomes a physically cross-linked hydrogel with the formation of an infinite gelatin molecular network. Moreover, when the temperature rises above 35 °C, such a gelatin hydrogel can gradually change into the sol.[27] Hence, in our case, the viscous mixture of gelatin aqueous solution and CDDP-loaded GEL-PAA nanoparticle suspension can form the hydrogel (CDDP-NP-Jelly) when stored at 4 °C. On the basis of this property, the CDDP-NP-Jelly can be made in any shape and size to better fit the tumor surface. To study the *in vitro* physical state, stability, and aqueous solubility of the CDDP-NP-Jelly at 37 °C, the CDDP-NP-Jelly in a gel state that was made of 40% gelatin solution (CDDP-loaded nanoparticle loading content of 0.6%) was placed into PBS solution and stored at 37 °C. As shown in Figure 2A, CDDP-NP-Jelly gradually becomes a sol with high viscosity and poor fluidity in PBS solution at 37 °C within 60−70 min. In addition, after the gel−sol transition, the PBS solution gradually changes from clear to bluish, implying that the gelatin molecules and the nanoparticles in the viscous sol can diffuse into the PBS solution from the sol/PBS interface. Then the supernatant PBS was sampled and monitored by TEM (Figure S2 in the Supporting Information). It is found that a large number of nanoparticles with a size of about 90 nm are observed, confirming the release of nanoparticles from the jelly. This may be because both the nanoparticles and gelatin molecules are negatively charged in the sol (pH 5.5−6.5), which stabilizes the nanoparticles through electrostatic repulsion.

To investigate the *in vitro* release profile of CDDP-loaded GEL-PAA nanoparticles from the jelly at 37 °C, at designated time intervals, the supernatant PBS solution was centrifuged to remove the free gelatin molecules and then the weight of the released nanoparticles was determined. As shown in Figure 2B, during the gel−sol transition of the initial 1 h, only about 7% of the nanoparticles are released. However, after the formation of the viscous sol, the nanoparticles were released rapidly from the sol, that is, around 80% of the nanoparticles can be released in 5 h. It is also noted that the release profile for nanoparticles from the jelly can be easily modulated by changing the gelatin concentration of the jelly (Figure S3 in the Supporting Information). In comparison, the CDDP-loaded GEL-PAA nanoparticles were also incorporated into the freeze-dried and chemically cross-linked gelatin hydrogel that is well documented for controlled release of anticancer drugs.[14,15] However, no nanoparticles with a size of around 90 nm can be detected in the supernatant PBS solution even after 24 h. Thus, compared to the freeze-dried and chemically cross-linked gelatin hydrogel, the physically cross-linked jelly more easily releases the encapsulated nanoparticles.

The *in vitro* release of CDDP from CDDP-NP-Jelly was also examined. In media containing chloride ions, the CDDP can be released *via* the exchange reaction between the chloride ions and carboxylic group of the GEL-PAA nanoparticles.[26] Figure 2C depicts the cumulative *in vitro* CDDP release profiles up to 5 d of CDDP-loaded nanoparticles and CDDP-NP-Jelly in PBS at 37 °C. It can be seen that both the nanoparticles and CDDP-NP-Jelly show sustained release behaviors for CDDP and the CDDP release is slower for the CDDP-NP-Jelly than that for nanoparticles within 5 d monitoring duration.

***In Vitro* Cellular Cytotoxicity Assays.** To assess the antitumor effect of the CDDP-loaded GEL-PAA nanoparticles, *in vitro* cytotoxicity against cultured human gastric carcinoma MKN-28 cells was initially assayed (Figure 3A). It is found that the CDDP-loaded nanoparticles

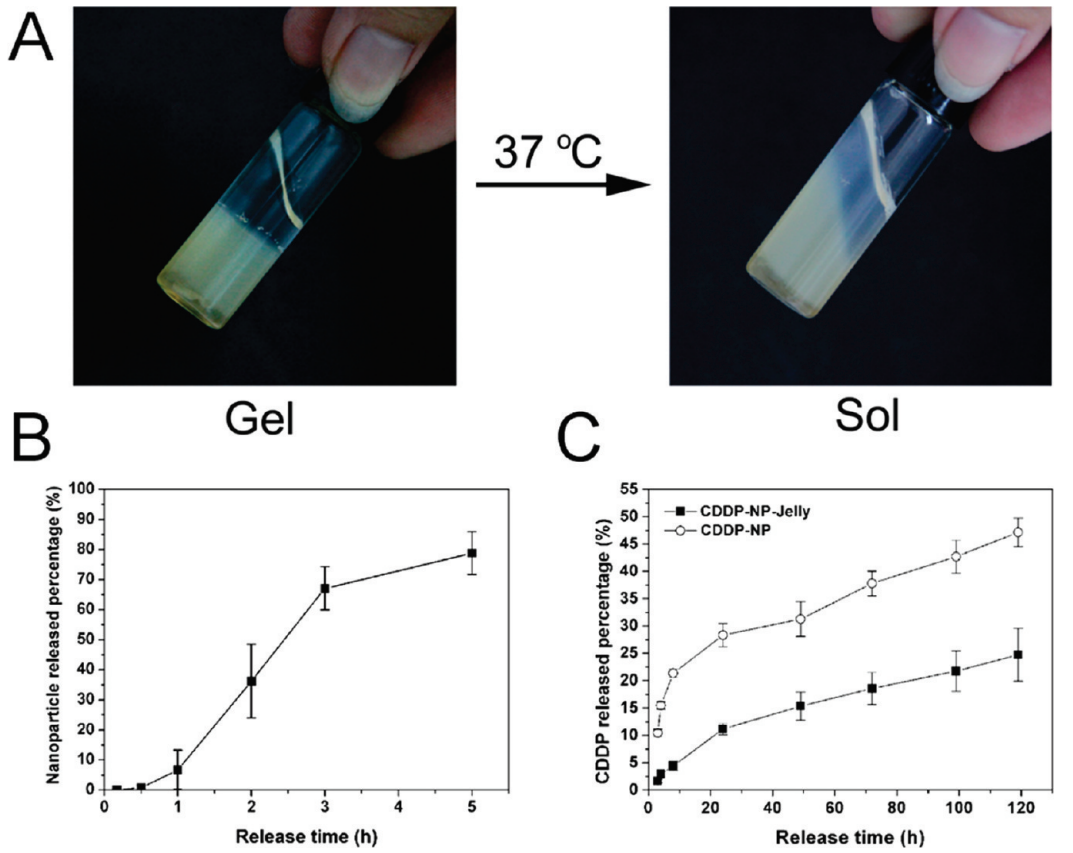

Figure 2. (A) Images of CDDP-NP-Jelly in PBS solution that undergoes a gel−sol transition at 37 °C. (B) *In vitro* release profile of CDDP-loaded GEL-PAA nanoparticles from the jelly in PBS at 37 °C. (C) *In vitro* release profiles of CDDP from the CDDP-NP-Jelly and GEL-PAA nanoparticles in PBS at 37 °C.

display similar cytotoxic activity to free CDDP at all tested concentrations. The IC_{50} values of free CDDP and CDDP-loaded GEL-PAA nanoparticles against MKN-28 cells are 3.1 and 2.8 μg/mL, respectively. It is also revealed that empty nanoparticles are nontoxic even at the highest concentration (1 mg/mL, Figure S4 in the Supporting Information). The cytotoxicity of drug-loaded nanoparticles against H_{22} cells was also investigated by the same method as that for MKN-28 cells, which demonstrated again the similar cytotoxicity between CDDP-loaded nanoparticles and free CDDP (Figure 3B). The IC_{50} is 2.2 μg/mL for free CDDP and 2.5 μg/mL for nanoparticles against H_{22} cells. In addition, in another cytotoxicity test, MKN-28 cells were exposed to the same doses of free CDDP and CDDP-NP-Jelly at 37 °C for 48 h as well (Figure 3C). It is found that the cytotoxicity of CDDP-NP-Jelly is lower than that of free CDDP over a range of experimental concentrations because of the slow but sustained release of CDDP form CDDP-NP-Jelly (IC_{50} values: 3.3 μg/mL for free CDDP and 9.1 μg/mL for CDDP-NP-Jelly). Laser scanning confocal microscopy (LSCM) was used to trace the cellular uptake of CDDP-loaded nanoparticles that were labeled by rhodamine B isothiocyanate (RBITC). After 2 h of incubation of MKN-28 cells with the nanoparticles at 37 °C, the normal morphology of the cells was still maintained and fluorescence was localized mainly in the cell cytoplasm (Figure 3D), demonstrating that the CDDP-loaded nanoparticles can readily penetrate the cell membrane barrier and reach the cell cytoplasm.

***In Vivo* Antitumor Efficacy.** In this study, murine hepatic H_{22} tumor-bearing ICR mice were used as the model animals to study the *in vivo* antitumor effect of CDDP-NP-Jelly. The CDDP-NP-Jelly was surgically coated on the surface of the tumor as described in the experimental section. It is noteworthy that the jelly has not changed into a sol while still maintaining its hydrogel state during the whole surgical process. Afterward, the jelly gradually transforms into the viscous sol *in vivo* due to the body temperature (>35 °C) (Scheme 2), as demonstrated in Figure 2A. Moreover, it is found that the viscous sol disappears around the tumor site in about 8 h after the implantation, implying that the viscous sol containing CDDP-loaded nanoparticles (CDDP concentration of 6 mg/kg) has almost diffused into the tumor tissue.

The *in vivo* antitumor efficacy of CDDP-NP-Jelly was then examined. As a comparison, the antitumor efficacies of other formulations of CDDP with different administration manners, including CDDP-loaded nanoparticles with i.v. administration (CDDP-NP-i.v.),

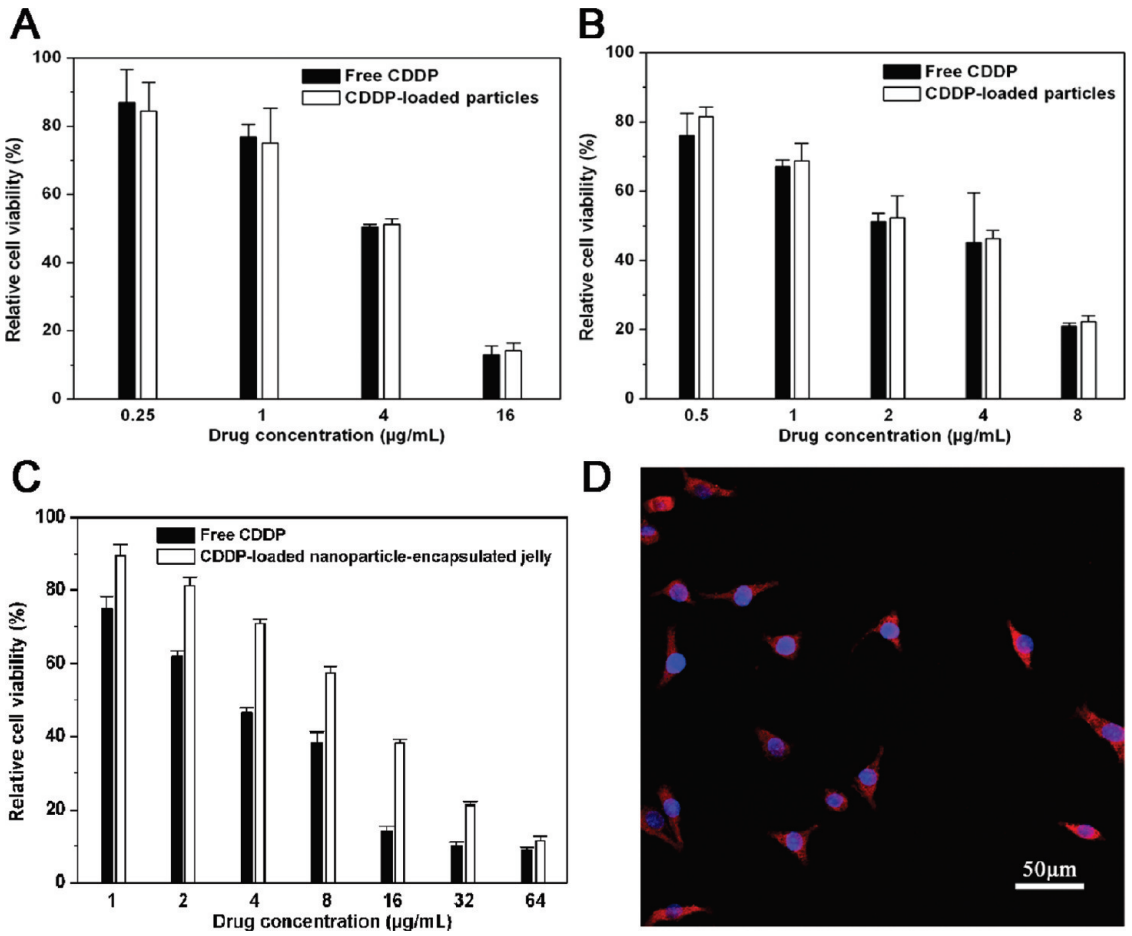

Figure 3. (A) *In vitro* cytotoxicity of free CDDP and CDDP-loaded nanoparticles against MKN-28 cells at 48 h. (B) *In vitro* cytotoxicity of free CDDP and CDDP-loaded nanoparticles against H_{22} cells at 48 h. (C) *In vitro* cytotoxicity of free CDDP and CDDP-NP-Jelly against MKN-28 cells at 48 h. (D) LSCM image of MKN-28 cells incubated with CDDP-loaded nanoparticles that were labeled by RBITC, at 37 °C for 2 h. The cell nuclei were stained by Hoechst 33258 (blue).

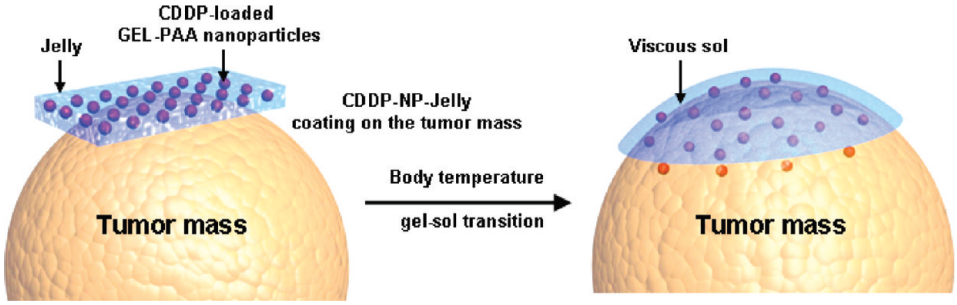

Scheme 2. Schematic illustration of CDDP-NP-Jelly coating on the tumor, which gradually transforms into a viscous sol *in vivo* due to the body temperature.

CDDP-containing jelly with surgical coating (CDDP-Jelly), CDDP with i.v. administration (CDDP-i.v.), empty nanoparticle-containing jelly with surgical coating (NP-Jelly), and saline with i.v. administration, were also examined. Thus, the animals for antitumor efficacy examination were divided into six groups, and each group contained six mice. The CDDP dose for examination was 6 mg/kg on a CDDP basis. The change in tumor size of mice was trailed for 15 days. It is notable that the administration of CDDP-NP-Jelly with subcutaneously coating the tumor, like a "plaster" through a surgical skin incision, is much more efficacious in tumor suppression compared with the CDDP-NP-i.v. group and other groups (Figure 4A). The tumor growth almost completely stops after the administration of CDDP-NP-Jelly.

It is also found that no antitumor effect is observed in the groups of saline and NP-Jelly, and the mean tumor volumes at the termination of the study for the groups are 9599 and 8849 mm^3, respectively. All of the

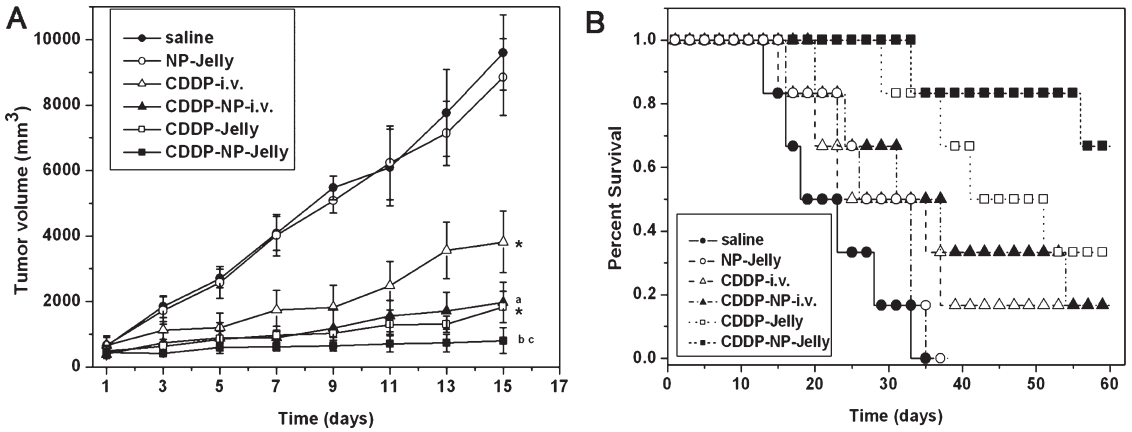

Figure 4. Antitumor effect in H_{22} subcutaneous model. (A) Tumor volume of established H_{22} xenografts in ICR mice that received different treatments indicated. The same CDDP dose (6 mg/kg) was administered on day 1 for CDDP-i.v., CDDP-NP-i.v., CDDP-Jelly, and CDDP-NP-Jelly groups. Data are presented as mean ± SD (n = 6). * represents $P < 0.01$ versus the saline group, "a" represents $P < 0.05$ versus CDDP-i.v. group from the 7th day, "b" represents $P < 0.01$ versus CDDP-Jelly group from the 7th day, "c" represents $P < 0.01$ versus CDDP-NP-i.v. group from the 11th day. (B) Survival rates of tumor-bearing mice treated with different protocols indicated.

animals in saline- and NP-Jelly-treated groups died within 36 days (Figure 4B), and this observation agrees well with the considerably fast growth rate of H_{22} tumor in ICR mice.[28] The CDDP-i.v. group exhibits an antitumor efficacy to some extent, and the tumor size for the CDDP-i.v.-treated group is much smaller than that of the saline- and NP-Jelly-treated groups ($P <$ 0.01). However, only one mouse in the CDDP-i.v. group survived 60 days. CDDP-NP-i.v. is more efficacious for tumor inhibition than CDDP-i.v., and the difference in tumor volume between these two groups is statistically significant ($P < 0.05$) from day 7. Similar to CDDP-i.v. group, five of the six mice died in the CDDP-NP-i.v. group within 60 days, but the median survival time for the CDDP-NP-i.v.-treated group is slightly longer than that for the CDDP-i.v.-treated group. The antitumor efficacy of CDDP-Jelly is similar to that of CDDP-NP-i.v. The mean tumor size of the CDDP-Jelly group and CDDP-NP- i.v. group at the final test point is 1836 and 1975 mm^3, respectively.

Notably, the CDDP-NP-Jelly group exhibits the most dramatic antitumor efficacy. The mean tumor volume at the end point is 805 mm^3, significantly smaller than that of other groups. In detail, five of the six treated mice underwent complete tumor inhibition during the initial 15-day duration with a mean tumor size of 628 mm^3, in contrast to the initial tumor volume of 447 mm^3 when administered. The remaining one mouse also efficiently suppressed tumor growth compared with other groups on day 15. More importantly, four of the six mice experienced slight tumor growth and even a growth stoppage from day 15 to day 60. Two of the six mice in this group died within 60 days, one of which died on day 57. The antitumor effect of the CDDP-NP-Jelly group is significantly superior to the CDDP-Jelly group and the CDDP-NP-i.v. group ($P < 0.01$ from day 7 and day 11 respectively).

Through determining the tumor volume doubling time and the tumor inhibition rates on the 7th and 15th day, the pharmacodynamic variables of antitumor response to the therapy were investigated (Table S1 in the Supporting Information). The tumor volume doubling time for the CDDP-i.v. group is 5.3 days, compared with 3.6 days for the saline group. What is the most striking is that the tumor volume doubling time is high up to 22.5 days when treated with CDDP-NP-Jelly, which is significantly different from that of the CDDP-NP-i.v. and CDDP-Jelly groups (6.0 and 7.3 days, respectively, both $P < 0.01$). Similarly, remarkably better tumor inhibition rates are observed for the CDDP-NP-Jelly group on the 7th and 15th day as compared with the other groups. These results demonstrate that the CDDP-NP-Jelly formulation possesses the highest antitumor efficacy over other formulations, greatly prolonging the lifetimes of tumor-bearing mice.

Drug Accumulation and Biodistribution in Tumors and Organs. To explore the reason the CDDP-NP-Jelly formulation has the highest antitumor efficacy among the formulations we used, the pharmacokinetics and biodistribution of CDDP in ICR mice bearing H_{22} tumor xenograft were studied after administrating CDDP-i.v., CDDP-NP-i.v., CDDP-Jelly, and CDDP-NP-Jelly, which were carried out through determining platinum contents in tissues and blood by ICP-MS. The results are expressed as percentage of dose/g of wet tissue or dose/mL of blood at each test point. As shown in Figure 5, after i.v. administration, CDDP-loaded nanoparticles show longer blood circulation over free CDDP, indicated by 0.77 ± 0.20% versus 0.32 ± 0.04% dose/mL of nanoparticles versus free CDDP at 12 h post-administration ($P < 0.05$). Additionally, the accumulation of CDDP resulting from the i.v. administration of nanoparticles at the tumor site is much higher than that of free CDDP formulation, which cause a 3.3-fold and

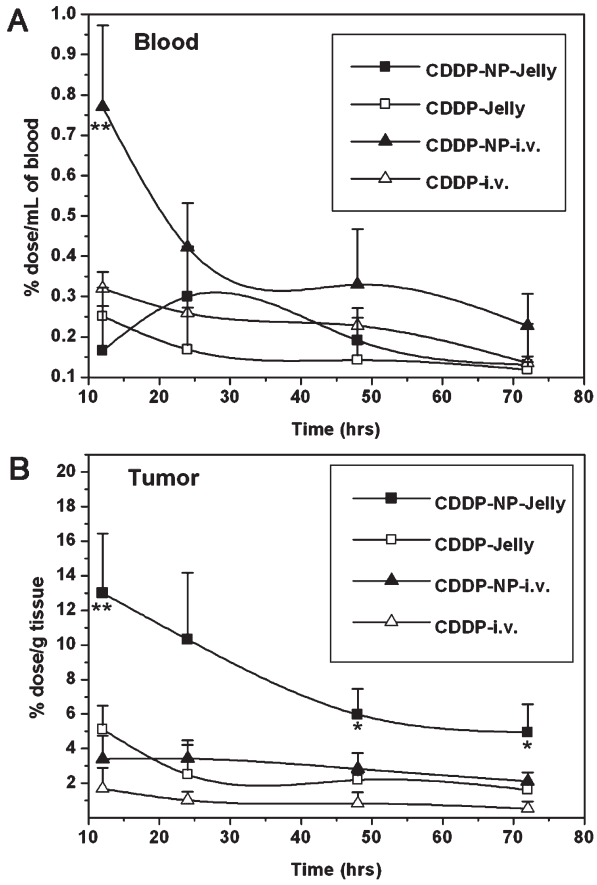

Figure 5. Time profiles of platinum concentration in plasma (A) and platinum accumulation in tumor (B) after various treatments indicated (CDDP dose, ~6 mg/kg). * and ** represent statistical significance ($P < 0.05$ and $P < 0.01$, respectively) between CDDP-NP-Jelly group and CDDP-NP-i.v. group. Data are presented as mean ± SD ($n = 4$).

3.4-fold increase in platinum level at 24 and 48 h, respectively ($P < 0.05$), as well as a 3.9-fold increase at 72 h ($P < 0.01$). Comparing CDDP-NP-Jelly and CDDP-NP-i.v., the platinum concentration in plasma for CDDP-NP-Jelly reaches a maximum at 24 h but is far lower than that of CDDP-NP-i.v. over the time period studied. For example, the platinum concentration in plasma for CDDP-NP-Jelly is 4.6-fold lower than that for CDDP-NP-i.v. at 12 h post-administration ($P < 0.01$). On the contrary, it is more noteworthy that CDDP accumulation and retention at the tumor site resulting from jelly administration remains significantly higher than that of systemic administration (Figure 5B). For instance, CDDP-NP-Jelly not only exhibits the maximal accumulation at 12 h, that is, 3.8-fold more platinum resides in the tumor tissue (12.99 ± 3.44% versus 3.40 ± 1.35% dose/g respectively, $P < 0.01$) but particularly shows 2.3-fold higher platinum retention at the tumor site at the termination of the study compared with CDDP-NP-i.v. (4.94 ± 1.63% versus 2.12 ± 0.51% dose/g, respectively, at 72 h, $P < 0.05$).

Different routes of administration may significantly change the biodistribution of a drug. An optimized biodistribution should be defined as not only enhanced drug potency but also reduced side effects.[29] Thereby, the CDDP distribution over time was evaluated in various organs so as to obtain a deeper insight into the *in vivo* behavior of the drug having varied administration routes (Figure 6). From the data of both i.v. administrations, the nanoparticle delivery shows a relatively increased drug accumulation in all of the organs in contrast to free CDDP at tested time points, especially in the liver and spleen of the mice. For implantation administrations, CDDP-NP-Jelly and CDDP-Jelly groups, the peak concentrations of platinum that accumulate in the examined tissues of the CDDP-NP-Jelly group occur at 24 h post-administration and then decay over time, while the peak accumulations of the CDDP-Jelly group seem to take place at the initial time point. Interestingly, comparing CDDP-NP-Jelly and CDDP-NP-i.v., CDDP accumulates in major organs to a much lesser extent through jelly implantation over i.v. injection; for example, there is a highly significant difference for kidney accumulation between these two formulations at 12 h post-administration ($P < 0.01$). Similar differences are also observed in liver ($P < 0.05$), spleen ($P < 0.01$), and lung accumulation ($P < 0.05$) between the two methods of delivery at all tested time points. More encouragingly, the tumors exhibit significant accumulation of platinum over all of

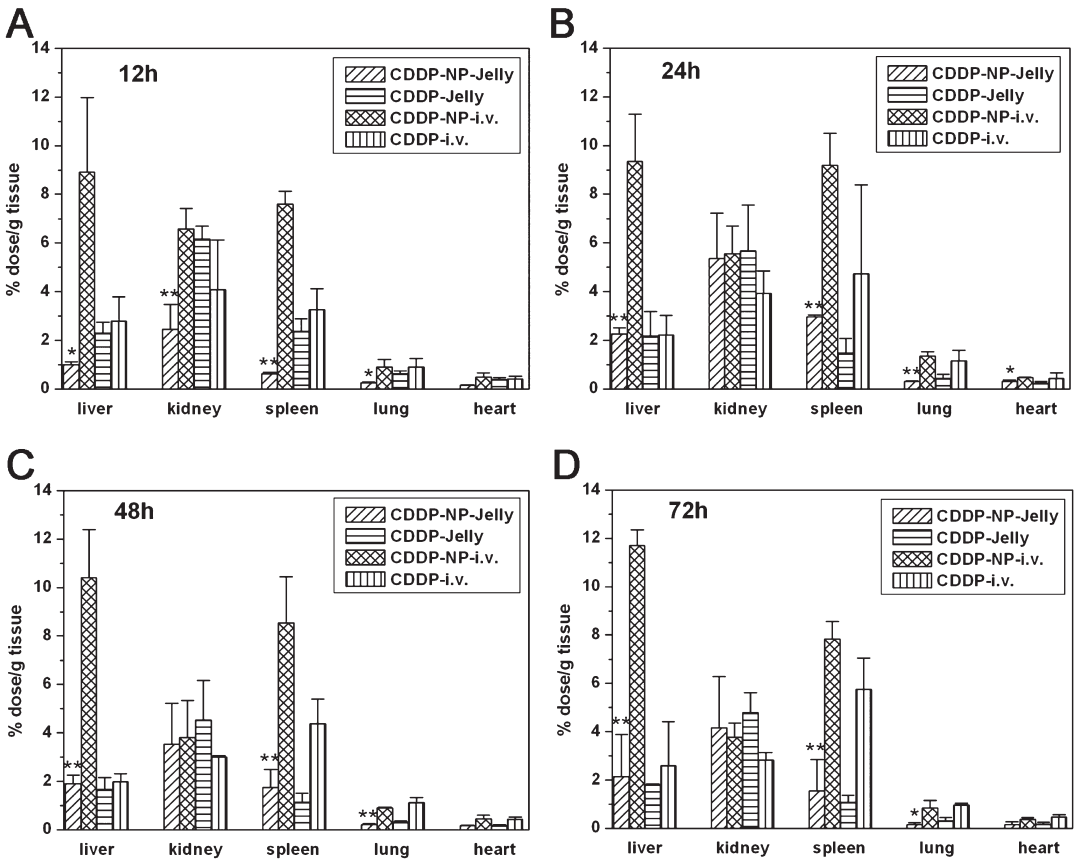

Figure 6. Biodistribution profiles of platinum accumulation in different organs of H_{22} tumor-bearing mice at 12 h (A), 24 h (B), 48 h (C), and 72 h (D) after different treatments indicated (CDDP dose, ~6 mg/kg). * and ** represent statistical significance ($P < 0.05$ and $P < 0.01$, respectively) between CDDP-NP-Jelly group and CDDP-NP-i.v. group. Data are presented as mean ± SD ($n = 4$).

the tested tissue types for the CDDP-NP-Jelly group by 12 h ($P < 0.01$) post-administration, especially for liver and spleen by 24 h ($P < 0.05$) and 48 h ($P < 0.05$) post-administration.

Systemic Toxicity Evaluation. Changes in body weights of tumor-bearing mice after administrations were evaluated to define the adverse effects of distinct therapy regimens (Figure 7A). Obviously, mouse body weights of the saline and NP-Jelly groups are higher than those of the other groups owing to the remarkable increases in tumor volumes. On the contrary, animals of the CDDP-i.v. group incur a slight body weight loss during the initial 7 days resulting from the severe side effects of CDDP. Although the body weights of the CDDP-NP-i.v.-treated mice are higher than those of the mice receiving systemic administration of CDDP, some animals in this group were in a weak state, showing, for example, a hunched posture and decreased activity, as all the mice in the CDDP-i.v. group did. It is noteworthy that the body weights of CDDP-NP-Jelly-treated mice are higher than those of mice in the CDDP-Jelly or CDDP-NP-i.v. group, and the mice presented an active state with respect to movement, spirit, and skin luster. A significant difference in the final body weights for the CDDP-NP-Jelly group compared with the CDDP-Jelly or CDDP-NP-i.v. group is observed (both $P < 0.05$), although the tumor sizes of CDDP-NP-Jelly-treated mice are pronouncedly smaller than those of the other two groups on day 15. In addition, H&E stained sections of some organs with platinum accumulation resulting from CDDP-NP-Jelly and CDDP-NP-i.v., including liver, kidney, and spleen, were investigated (Figure 7B). The images reveal that both of the treatments do not cause any abnormal damage in these organs. As a positive control, H&E stained kidney slices from mice treated with CDDP-i.v. suggest that this treatment results in nephrotoxicity to some extent, including tubular ectasia and hydropic degeneration of the epithelium (Figure S5 in the Supporting Information).

Penetration of Nanoparticles from Jelly into Tumor. For locoregional administration of jelly impregnated with CDDP-loaded GEL-PAA nanoparticles, to investigate the location of nanoparticles in the tumor and whether they can penetrate into the tumor interior, we treated the tumor-bearing mice with the jelly containing fluorescein isothiocyanate (FITC)-labeled and colloidal gold-encapsulated GEL-PAA nanoparticles (GEL-PAA-Au hybrid nanoparticles). After sacrificing the mice on day 1 post-administration, tumor sections were then monitored

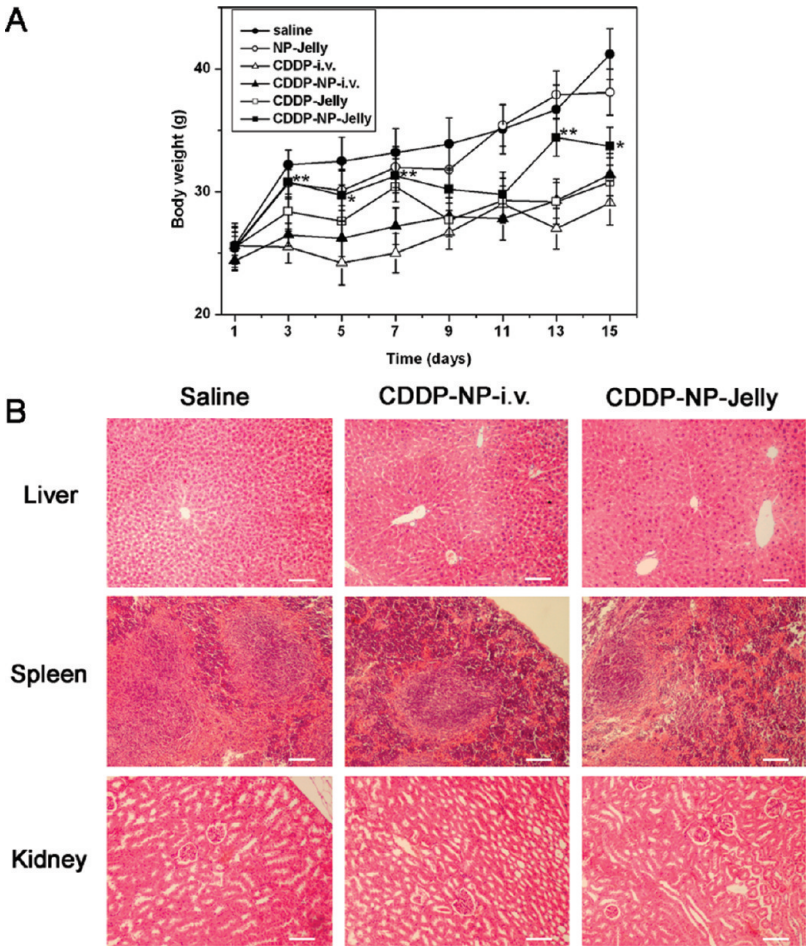

Figure 7. (A) Body weight change of mice receiving different treatments during therapy (CDDP dose, ~6 mg/kg). * and ** represent statistical significance ($P < 0.05$ and $P < 0.01$, respectively) between CDDP-NP-Jelly group and CDDP-NP-i.v. group. Data are presented as mean ± SD ($n = 6$). (B) H&E stained liver, spleen, and kidney slices from H_{22} tumor-bearing mice on the 15th day in CDDP-NP-i.v., CDDP-NP-Jelly, and saline groups. Scale bar, 100 μm.

by fluorescence microscopy in the FITC channel (Figure 8A). We observed fluorescently labeled GEL-PAA nanoparticles distributing at the edge of the tumor tissue in contrast to the control, suggesting that the nanoparticles have entered the tumor from the jelly/tumor interface by diffusion. We next examined the location of nanoparticles in relation to blood vessels in the tumor. However, FITC-labeled nanoparticles are hard to recognize clearly in the inner part of the tumor due to the sufficient disturbance of background autofluorescence of the tumor. Thus, dark-field optical microscopy of the jelly containing GEL-PAA-Au hybrid nanoparticles was conducted in the present work to evaluate whether these hybrid nanoparticles could appear relative to the vasculature. As shown in Figure 8B, some bright spots within the tumor attributed to the gold nanoparticles encapsulated inside the GEL-PAA nanospheres are clearly observed in the dark-field image both with and without overlaying with tumor vasculatures. It can be seen that most nanoparticles are distributed in or near the tumor vasculature, and some are located in the tumor interstitial space, suggesting that some nanoparticles can penetrate into the tumor inner portions, which are unreachable by simple diffusion alone, with the help of tumor vasculatures.

Furthermore, to verify the distribution of CDDP delivered by GEL-PAA nanoparticles in the tumor, we examined the effect of CDDP-loaded nanoparticles through both administration routes on H_{22} tumor cell apoptosis. The corresponding tumor samples were resected from the mice on day 2 post-administration, and the expression of cleaved caspase-3 was studied relative to the vasculature using immunohistochemical staining (Figure 8C). Qualitatively, cleaved caspase-3 positive cells in the CDDP-NP-Jelly and CDDP-NP-i.v. groups are explicitly much greater than those in saline and NP-Jelly groups. Additionally, images from the tumors treated with CDDP-NP-Jelly show that cleaved caspase-3 positive cells appear in the surface layer of the tumor, as expected. Besides, they are also localized around blood vessels in the other parts of the tumor slices, similar to the location in the CDDP-NP-i.v. group, suggesting the ability of CDDP-loaded nanopartcles from the jelly to penetrate into the interior of the tumor

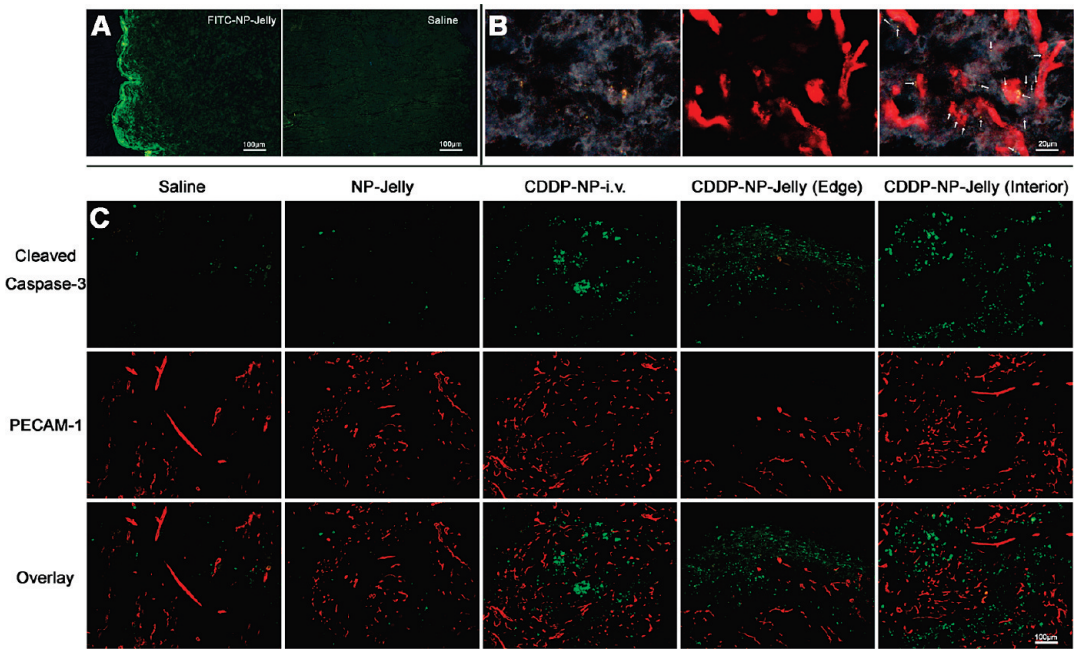

Figure 8. (A) Typical fluorescence microscopy images of tumor slices from mice treated with jelly impregnated with FITC-labeled nanoparticles (FITC-NP-Jelly) and saline. (B) Representative dark-field microscopy image of tumor slices from the mice treated with jelly containing GEL-PAA-Au hybrid nanoparticles. Tumor vasculature was stained by Alexa 594-anti-PECAM-1. Dark-field microscopy image was overlaid with vasculature fluorescence, showing the distribution of the clusters of GEL-PAA-Au hybrid nanoparticles (bright spots) in relation to blood vessels (red) in the interior of the tumor. The arrows indicate the location of bright spots. (C) Representative photos of immunohistochemical costaining against cleaved caspase-3 (green) and PECAM-1 (red) in different groups indicated. Tumors utilized in this study were taken from H_{22} tumor-bearing mice 1 d after initiation of administration for (A) and (B) as well as 2 d for (C).

through blood vessels once more for the implantation administration of CDDP-NP-Jelly.

DISCUSSION

Although each type of drug delivery system has its advantages and unresolved problems, the common challenges in the solid tumor treatment currently are to increase the ratio of drug in tumor to in normal tissue,[17,30] prolong drug exposure time at tumor sites,[11,14,31] and improve the drug penetration in tumor tissues and cells.[32−34] From our *in vivo* examinations, it is apparent that the peritumoral chemotherapy with the jelly containing CDDP-loaded nanoparticles is much more efficient in impeding tumor development (Figure 4A) and significantly less toxic to normal tissues than the other options we used. Compared to low drug concentration and rapid drug clearance for the CDDP-Jelly group, the high concentration and long retention time of CDDP in the tumor tissues for the CDDP-NP-Jelly group significantly demonstrate the sustained-release effect and delayed clearance from tumor arising from GEL-PAA nanoparticles, which also partially explains the reason we encapsulated the nanoparticles into the jelly. Thus, encapsulating the drug-loaded GEL-PAA nanoparticles into jelly becomes one of the features of the nanoparticle-encapsulated jelly system.

Comparing the local implantation administration of jelly containing CDDP-loaded nanoparticles with the i.v. administration of equivalent dosing of CDDP-loaded nanoparticles, the pharmacokinetic profiles of these two administrations are quite different. The amount of tumor accumulation of platinum administered as the jelly dramatically exceeds that of other groups at all of the tested time points, and even at the later stage of post-administration it is still nearly 3-fold higher than that of the CDDP-NP-i.v. group (Figure 5B), which may explain the reason for the superior *in vivo* anticancer efficacy of the CDDP-NP-Jelly group as well. It is also noteworthy that gelatin can dissolve in water above its melting temperature (about 35 °C) and form hydrogel (Jelly) upon cooling below the melting temperature, and change into a sol from the gel when the temperature rises above 35 °C.[27] In our case, the jelly maintains its hydrogel state during the whole surgical process with jelly coating on the tumor. Afterward, the jelly should gradually transform into a viscous sol *in vivo* due to the body temperature, as we observed in the *in vitro* test (Figure 2A), subsequently releasing the CDDP-loaded nanoparticles. Since our strategy is mainly to utilize the CDDP-loaded GEL-PAA nanoparticles for peritumoral chemotherapy with the help of jelly, the nanoparticles can be readily released from the jelly after it changes into a sol is the reason we selected the physically cross-linked gelatin hydrogel to replace the chemically cross-linked one as the nanoparticle reservoir. Thus, after transition into a sol *in vivo*, the drug-loaded nanoparticle-encapsulated jelly not only releases the encapsulated CDDP-loaded nanoparticles

but also forms a nanoparticle depot in the peritumoral region, offering a multipoint tumor-toward diffusion of the nanoparticles. This is the second feature of nanoparticle-encapsulated jelly system in our case.

In the present work, for i.v. administration, some nanoparticles can be taken up by reticuloendothelial system (RES) organs such as liver and spleen, attributed to their colloidal nature.[29,31] Moreover, since only a small amount of the systemic blood flow is directed to the tumor,[6] only a fraction of the total drug-loaded nanoparticles can arrive at the target through the enhanced permeability and retention (EPR) effect. Therefore, it is difficult to expect a high concentration of CDDP in the tumor tissue with i.v. adminstration. On the other hand, the implantation administration of jelly is a site-specific delivery, which makes enough nanoparticles administered in jelly appear to substantially enter the tumor tissue. Because far more nanoparticles could stay in the tumor for a longer time, ascribed to the impaired lymphatic system,[35] taking into consideration the sustained-release behavior of the CDDP-loaded nanoparticles, a longer time exposure of the tumor cells to CDDP can be carried out with the aid of nanoparticles from jelly. In addition, the relatively lower platinum level in plasma by local nanoparticle delivery, contrasted to i.v. administration (Figure 5A), means much less toxicity to normal tissues.

The distribution profiles of platinum in nonspecific target tissues show that nanoparticle administration in jelly significantly lowers the drug accumulation in normal tissues over that of nanoparticle delivery *via* i.v. injection (Figure 6). The lower toxicity may explain the relatively higher mean body weight (Figure 7A) but markedly smaller mean tumor volume and more active state of CDDP-NP-Jelly-treated mice throughout the study than those of mice in the CDDP-NP-i.v. group. It is well known that one of the side effects of CDDP is acute nephrotoxicity, which may be associated with its rapid and high accumulation in the kidney. Kataoka and colleagues found that after i.v. administration of free CDDP in C57BL/6N mice bearing Lewis lung carcinoma xenografts, almost 16% dose/g accumulation of platinum was observed in the kidney within 15 min.[36] However, for the nanoparticle delivery *via* jelly implantation, kidney uptake of platinum is very slow and reaches a plateau with a relatively low magnitude at about 24 h post-administration, which may efficiently reduce the nephrotoxicity of drug. In particular, it is noted that administration of CDDP-NP-Jelly results in a several-fold decreased uptake by RES organs in contrast to i.v. injection of nanoparticles. Hence, our data suggest that drug administration as nanoparticles *via* jelly implantation significantly alters the biodistribution of the drug. Thus, the jelly formulation does benefit nanoparticle delivery by remarkably elevating drug levels as well as prolonging drug retention in the tumor tissue and, at the same time, by greatly altering drug biodistribution with decreasing accumulation in nontarget organs, resulting in reduced side effects.

The results of nanoparticle penetration in tumors *via* jelly formulation clearly reveal that not only do the drug-loaded nanoparticles permeate the tumor tissue by diffusion but also they are able to penetrate the tumor deeply through leaky tumor vasculature (Figure 8). A portion of nanoparticles entering the tumor may be transported by either diffusion or convection into the nearby blood vessels.[37] This implies that some particles do not pass into blood circulation, whereas they tend to passively extravasate through the leaky blood vessels in the tumor where the blood flow reaches. It is well known that the tumor microenvironment such as increased interstitial fluid pressure (IFP) and extracellular matrix (ECM) hamper drug permeation in the tumor interior.[38] In our case, although the size of the nanoparticles (about 100 nm) does not favor nanoparticle penetration in the ECM very efficiently,[35,39] the drug-loaded nanoparticles in the CDDP-NP-Jelly group can be distributed in the tumor not only by diffusion but also by the help of leaky tumor vasculature into the tumor interior, enabling the released drug to efficiently reach more viable cells of the tumor over i.v. injected nanoparticles. The drug distribution for the CDDP-NP-Jelly group is more homogeneous in the tumor than that of the CDDP-NP-i.v. group from the observation of tumor cell apoptosis (Figure 8C), suggesting that the drug penetration in the tumor is improved in the CDDP-NP-Jelly group, becoming the third feature of the nanoparticle-encapsulated jelly system. The remarkably increasing accumulation and retention of drug in the tumor and excellent affinity between gelatin nanoparticles and the ECM may explain the reason for such improved penetration.

From a clinical cancer therapy standpoint, the jelly is able to suitably attach to the surface of residual tumors and even any suspicious site immediately after debulking surgery, which may efficiently prevent from the recurrence caused by metastatic dissemination of remnant tumor tissues. Moreover, CDDP-NP-Jelly may be very suitable for the treatment of skin tumors. Encouragingly, it is noted that locoregional chemotherapy on the basis of biocompatible and biodegradable polymeric materials has been clinically used in the treatment of brain tumors since conventional systemic chemotherapy for brain tumors has been greatly limited by the blood–brain and blood–cerebrospinal fluid barriers.[40] Thus, our locoregional therapy strategy based on nanotechnology may hold great promise for the treatment of brain tumors and other tumors.

CONCLUSIONS

In this study, we incorporated CDDP-loaded GEL-PAA nanoparticles into the gelatin hydrogel to obtain a

nanoparticle-encapsulated jelly that can be implanted and plastered on the tumor surface in any shape. An *in vitro* cytotoxicity assay using MKN-28 and H_{22} cell lines revealed that CDDP-loaded nanoparticles could be readily internalized by the cells and had similar cytotoxicity to free CDDP. *In vivo* antitumor efficacy examinations indicated that the implantation of the nanoparticle-encapsulated jelly on tumor tissues possessed significantly superior efficacy in impeding tumor growth and prolonging the lifetime of mice than those treated with i.v. injection of CDDP-loaded nanoparticles due to higher concentration and retention of CDDP in the tumor and lower CDDP uptake in nontarget organs as well as more efficient drug penetration through the tumor resulting from jelly administration. Microscopically, the nanoparticles from the jelly could be distributed in tumor tissue not only by diffusion but also by the help of leaky tumor vasculature into the tumor interior, enabling CDDP to efficiently reach more viable cells of the tumor compared with i.v.-injected nanoparticles. Thus, it is reasonable to say that peritumoral chemotherapy based on hydrogel-containing nanoparticles is very promising for future cancer therapy.

METHODS AND EXPERIMENTS

Materials. Type-B gelatin (225 bloomstrength) with 100−115 mmol of carboxylic acid per 100 g of protein, an isoelectric point of 4.7−5.2, and an average molecular weight 40−50 kDa was purchased from Sigma-Aldrich (St Louis, MO). Potassium persulfate ($K_2S_2O_8$) was recrystallized from deionized water before use. Acrylic acid (AA) (Guanghua Chemical Company, Shanghai, China) was distilled under reduced pressure in nitrogen atmosphere. 2,2′-(Ethylenedioxy)bis(ethylamine), *N*-(3-dimethylaminopropyl)-*N*′-ethylcarbodiimide hydrochloricde (EDC), and 1-(4,5-dimethylthiazol-2-yl)-3,5-diphenylformazan (MTT) were purchased from Aldrich. Fluorescein isothiocyanate (FITC) and rhodamine B isothiocyanate (RBITC) were purchased from Shenggong Company (Shanghai, China). Cisplatin (CDDP) was provided by Jiangsu Hengrui Pharmaceutical Co. Ltd. (Lianyungang, China). All other reagents were of analytical grade and used without further purification. Human gastric carcinoma cell line MKN-28 and murine hepatic carcinoma cell line H_{22} were purchased from Shanghai Institute of Cell Biology (Shanghai, China). Male ICR mice (6−8 weeks old) were purchased from Animal Center of Drum-Tower Hospital (Nanjing, China).

Preparation of GEL-PAA Nanoparticles. Purified gelatin (0.8 g) was dissolved in 50 mL of acrylic acid (0.2 g) aqueous solution, and then the polymerization of AA monomer was initiated by $K_2S_2O_8$ at 80 °C. As the opalescence appeared in the reaction mixture, which was a signal of the formation of gelatin-PAA nanoparticles, the reaction was allowed to proceed for another 120 min at 80 °C. The resultant suspension was then filtered with filter paper to remove any larger aggregation and dialyzed against a buffer solution of pH 3.0 for 24 h using a dialysis membrane bag (12 kDa cutoff) to remove residual monomers and other residual molecules. After this, the cross-linking reaction of the nanoparticles was conducted by adding 2,2′-(ethylenedioxy)bis(ethylamine) as cross-linker in the presence of EDC at room temperature for 12 h. The molar ratio of amine groups in the cross-linker to carboxylic groups of the nanoparticles was kept at 0.5:1 (except when otherwise stated). The cross-linked product was again dialyzed against distilled water for 24 h.

For the measurement of the molecular weight of PAA during the polymerization, GEL-PAA nanoparticles synthesized with different reaction time from 30 to 150 min were separated from the solution by centrifugation at 15 000 rpm for 30 min. Then the sediments were dissolved by an aliquot of 0.2 M Na_2CO_3/$NaHCO_3$ buffer. The resultant solutions were subject to molecular weight measurement by a gel permeation chromatography system (GPC) equipped with a static light-scattering detector (Dawn Heleos, Wyatt Technology Corporation) so that the absolute molecular weight of the PAA could be obtained.

Preparation of CDDP-Loaded GEL-PAA Nanoparticles. CDDP was dissolved in a gelatin-PAA nanoparticle suspension (4.22 mg/mL) at 1 mg/mL, which was allowed to proceed at 37 °C for 2 days. Then this suspension was treated with the method developed by Kataoka's group to remove free drug.[26] The Pt content in the particles was measured by ion coupled plasma-mass spectrometry (ICP-MS, Perkin-Elmer Corporation, USA).

Preparation of CDDP-Loaded Nanoparticle-Encapsulated Jelly. Gelatin powder was dissolved in distilled water at 45 °C for 1 h to prepare a gelatin solution with 40 wt % concentration. Then the gelatin solution was mixed with a CDDP-loaded GEL-PAA nanoparticle suspension or free CDDP solution to make a viscous mixture with a CDDP concentration of 1 mg/mL. The desired amount of the resulting solution was cast into plastic wells of a 24-well cell culture plate, and the hydrogel (jelly) was subsequently fabricated and stored at 4 °C until use. The CDDP-loaded nanoparticle loading content was expressed by the ratio of the weight of CDDP-loaded nanoparticles in CDDP-NP-Jelly to that of the CDDP-NP-Jelly. To study the *in vitro* physical state, stability, and aqueous solubility of the CDDP-NP-Jelly at 37 °C, the CDDP-NP-Jelly was placed into 1× PBS solution and stored at 37 °C.

***In Vitro* Nanoparticle Release from the Jelly.** The prepared CDDP-NP-Jelly (made of 1 mL mixture) was placed into 1 mL of 1× PBS solution and kept in an incubator at 37 °C. At designated time intervals, the supernatant PBS solution was washed and centrifuged with distilled water three times to remove the free gelatin molecules (35 000 rpm, 15 min). Then the weights of released nanoparticles at different time points were determined. The nanoparticle released percentage (NRP) was calculated as NRP = weight of released nanoparticles/weight of nanoparticles in jelly before release × 100%.

***In Vitro* CDDP Release from the Jelly.** The release profiles of CDDP from CDDP-NP-Jelly and GEL-PAA nanoparticles in 1× PBS at 37 °C was evaluated by the dialysis method.[28] Briefly, CDDP-NP-Jelly made of a 1 mL mixture was put into a dialysis bag (MWCO 12000). Then the bag was immersed into 15 mL of 1× PBS buffer and kept in an incubator at 37 °C. At designated time intervals, the PBS buffer was withdrawn for ICP-MS analysis, and equivalent fresh PBS buffer was added. A release study of CDDP form GEL-PAA nanoparticles was performed under the same conditions.

***In Vitro* Cytotoxicity Analysis.** Human gastric carcinoma cell line MKN-28 and murine hepatic carcinoma cell line H_{22} were cultured in the standard medium. Both cell types were seeded in 96-well plates with a density around 5000 cells/well. MKN-28 cells were allowed to adhere for 24 h prior to the assay. Then both cell types were co-incubated with a series of doses of free CDDP, empty nanoparticles, and CDDP-loaded nanoparticles at 37 °C for 48 h. Moreover, after the CDDP-loaded nanoparticle-encapsulated jelly had changed into a viscous sol at 37 °C, a series of doses of the samples were also added to the MKN-28 cells, which were then incubated at 37 °C for 48 h. Cell viability after different treatments was examined by the MTT assay as previously described.[28]

***In Vivo* Anticancer Efficacy.** All animal studies were performed in compliance with guidelines set by the Animal Care Committee

at Drum-Tower Hospital. Male ICR mice implanted with murine hepatoma cell line H_{22} were used to investigate the antitumor effect of CDDP-loaded nanoparticles (i.v.) and CDDP-loaded nanoparticle-encapsulated jelly (implantation) as well as CDDP-loaded jelly (implantation). A 0.1 mL amount of cell suspension containing $(5-6) \times 10^6$ H_{22} cells was injected into the left axillary space of the ICR mice with an average body weight of 25 g. Various treatments were started when the tumor volume reached a mean size of about 500 mm^3. This day was designated as "day 1".

For jelly implantations, the mice were anesthetized with intraperitoneal injection of trichloroacetaldehyde hydrate solution (2.5% in saline, 0.2 mL per mouse) prior to surgery. After disinfecting, an about 1 cm skin incision was made beside the tumor mass. At this site, a subcutaneous pocket was created along the tumor mass, and the jelly was subsequently inserted and coated on the tumor. Then the skin wound was sutured with surgical sutures. On day 1, mice were randomly divided into six groups. Each group contains six mice. Jellies with CDDP, CDDP-loaded nanoparticles, and empty nanoparticles, respectively, were implanted into the mice. Another two groups of mice were treated i.v. with free CDDP and CDDP-loaded nanoparticles, respectively. Saline was used in control experiments. The same CDDP dose (6 mg/kg) was administered for CDDP-i.v., CDDP-NP-i.v., CDDP-Jelly, and CDDP-NP-Jelly groups. Tumors were measured by a caliper every other day, and the volume (V) was calculated as $V = W^2 \times L/2$, where W and L are width and length of the tumor, respectively. Animals were also weighed every other day, and the survival rates were monitored throughout the study.

Biodistribution Examination *in Vivo*. ICR mice bearing H_{22} tumors were randomly assigned to four groups ($n = 16$ mice per group) and treated with CDDP-i.v., CDDP-NP-i.v., CDDP-Jelly, and CDDP-NP-Jelly, respectively, at a dose of 6 mg/kg on a CDDP basis. In each group, the animals were sacrificed at 12, 24, 48, and 72 h after administration ($n = 4$ at each time point). Subsequently, the tumor, liver, spleen, kidney, lung, and heart were excised, and blood was collected, heparinized, and centrifuged to obtain the plasma. The Pt concentration measurement in these organs and plasma was based on a method reported by Kataoka's group.[41] The samples were decomposed on heating in nitric acid. After being evaporated to dryness, they were dissolved in 2 N hydrochloric acid solution. Then the Pt concentration in the solution was measured by ICP-MS. The data were normalized to the tissue weight.

Histology Observation. The tissues including liver, spleen, and kidney from the mice that received CDDP-NP-i.v., CDDP-NP-Jelly, and saline were selected for histology observation on the 15th day after treatment ($n = 3$ mice per group). The organs were dissected and fixed in 10% neutral buffered formalin. Thereafter, the tissues were processed routinely into paraffin, sectioned at a thickness of 4 μm, and stained with hematoxylin and eosin (H&E). The slices obtained were examined by optical microscopy.

Labeling of CDDP-Loaded GEL-PAA Nanoparticles. The experimental details for the preparation of FITC/RBITC-labeled nanoparticles and colloidal gold-encapsulated GEL-PAA nanoparticles (GEL-PAA-Au) hybrid nanoparticles can be found in the Supporting Information.

Penetration in Tumor Tissue: Imaging and Staining of Tumor Slices. The tumor slice was taken as a cross-section through the center of the whole tumor mass and monitored by fluorescence microscopy or dark-field optical microscopy, as well as stained with standard fluorescent PECAM-1 and Cleaved Caspase-3 staining procedures (see details in the Supporting Information).

Statistical Analysis. Quantitative data were expressed as mean $\pm$ SD. Statistical comparisons were made by ANOVA analysis and Student's t-test. A P value < 0.05 was considered statistically significant.

Acknowledgment. This study was supported by National Natural Science Foundation of China (No. 51033002, 50625311, 20874042) and the New Drug Preparation Program of MOST (Grant 2009ZX09503-028). Thanks are given to Prof. Yulong He, Model Animal Research Institute, Nanjing University, for technical assistance in slice production and immunohistochemical examination.

Supporting Information Available: Experimental details for labeling of nanoparticles and imaging and staining of tumor slices, figures depicting TEM images of cross-linked nanoparticles and the nanoparticles released from jelly, *in vitro* release profiles of nanoparticles from jelly, cytotoxicity of empty nanoparticles, as well as H&E stained images from mice treated with CDDP-i.v., and table showing tumor volume doubling time and inhibition rate. This material is available free of charge *via* the Internet at http://pubs.acs.org.

REFERENCES AND NOTES

1. Gref, R.; Minamitake, Y.; Peracchia, M. T.; Trubetskoy, V.; Torchilin, V.; Langer, R. Biodegradable Long-Circulating Polymeric Nanospheres. *Science* **1994,** *263*, 1600–1603.
2. Sengupta, S.; Eavarone, D.; Capila, I.; Zhao, G. L.; Watson, N.; Kiziltepe, T.; Sasisekharan, R. Temporal Targeting of Tumour Cells and Neovasculature with a Nanoscale Delivery System. *Nature* **2005,** *436*, 568–572.
3. Kim, J. H.; Kim, Y. S.; Park, K.; Kang, E.; Lee, S.; Nam, H. Y.; Kim, K.; Park, J. H.; Chi, D. Y.; Park, R. W.; *et al.* Self-Assembled Glycol Chitosan Nanoparticles for the Sustained and Prolonged Delivery of Antiangiogenic Small Peptide Drugs in Cancer Therapy. *Biomaterials* **2008,** *29*, 1920–1930.
4. van Vlerken, L. E.; Duan, Z.; Little, S. R.; Seiden, M. V.; Amiji, M. M. Biodistribution and Pharmacokinetic Analysis of Paclitaxel and Ceramide Administered in Multifunctional Polymer-Blend Nanoparticles in Drug Resistant Breast Cancer Model. *Mol. Pharmaceutics* **2008,** *5*, 516–526.
5. Farokhzad, O. C.; Langer, R. Impact of Nanotechnology on Drug Delivery. *ACS Nano* **2009,** *3*, 16–20.
6. Dowell, J. A.; Sancho, A. R.; Wolf, W. Noninvasive Measurements for Studying the Tumoral Pharmacokinetics of Platinum Anticancer Drugs in Solid Tumors. *Adv. Drug Delivery Rev.* **2000,** *41*, 111–126.
7. Liu, Z.; Chen, K.; Davis, C.; Sherlock, S.; Cao, Q. Z.; Chen, X. Y.; Dai, H. J. Drug Delivery with Carbon Nanotubes for *In Vivo* Cancer Treatment. *Cancer Res.* **2008,** *68*, 6652–6660.
8. Minchinton, A. I.; Tannock, I. F. Drug Penetration in Solid Tumours. *Nat. Rev. Cancer* **2006,** *6*, 583–592.
9. Nagano, S.; Perentes, J. Y.; Jain, R. K.; Boucher, Y. Cancer Cell Death Enhances the Penetration and Efficacy of Oncolytic Herpes Simplex Virus in Tumors. *Cancer Res.* **2008,** *68*, 3795–3802.
10. Kim, K. Y. Nanotechnology Platforms and Physiological Challenges for Cancer Therapeutics. *Nanomed.: Nanotechnol., Biol., Med.* **2007,** *3*, 103–110.
11. Farokhzad, O. C.; Cheng, J. J.; Teply, B. A.; Sherifi, I.; Jon, S. Y.; Kantoff, P. W.; Richie, J. P.; Langer, R. Targeted Nanoparticle-Aptamer Bioconjugates for Cancer Chemotherapy *In Vivo*. *Proc. Natl. Acad. Sci. U. S. A.* **2006,** *103*, 6315–6320.
12. van Etten, B.; ten Hagen, T. L.; de Vries, M. R.; Ambagtsheer, G.; Huet, T.; Eggermont, A. M. Prerequisites for Effective Adenovirus Mediated Gene Therapy of Colorectal Liver Metastases in the Rat Using an Intracellular Neutralizing Antibody Fragment to p21-Ras. *Br. J. Cancer* **2002,** *86*, 436–442.
13. McKee, T. D.; Grandi, P.; Mok, W.; Alexandrakis, G.; Insin, N.; Zimmer, J. P.; Bawendi, M. G.; Boucher, Y.; Breakefield, X. O.; Jain, R. K. Degradation of Fibrillar Collagen in a Human Melanoma Xenograft Improves the Efficacy of an Oncolytic Herpes Simplex Virus Vector. *Cancer Res.* **2006,** *66*, 2509–2513.
14. Konishi, M.; Tabata, Y.; Kariya, M.; Hosseinkhani, H.; Suzuki, A.; Fukuhara, K.; Mandai, M.; Takakura, K.; Fujii, S. *In Vivo* Anti-Tumor Effect of Dual Release of Cisplatin and Adriamycin from Biodegradable Gelatin Hydrogel. *J. Controlled Release* **2005,** *103*, 7–19.
15. Konishi, M.; Tabata, Y.; Kariya, M.; Suzuki, A.; Mandai, M.; Nanbu, K.; Takakura, K.; Fujii, S. *In Vivo* Anti-Tumor Effect through the Controlled Release of Cisplatin from Biodegradable Gelatin Hydrogel. *J. Controlled Release* **2003,** *92*, 301–313.

16. Emerich, D. F.; Snodgrass, P.; Lafreniere, D.; Dean, R. L.; Salzberg, H.; Marsh, J.; Perdomo, B.; Arastu, M.; Winn, S. R.; Bartus, R. T. Sustained Release Chemotherapeutic Microspheres Provide Superior Efficacy over Systemic Therapy and Local Bolus Infusions. *Pharm. Res.* **2002,** *19*, 1052–1060.
17. Okino, H.; Maeyama, R.; Manabe, T.; Matsuda, T.; Tanaka, M. Trans-Tissue, Sustained Release of Gemcitabine from Photocured Gelatin Gel Inhibits the Growth of Heterotopic Human Pancreatic Tumor in Nude Mice. *Clin. Cancer Res.* **2003,** *9*, 5786–5793.
18. Liu, J.; Meisner, D.; Kwong, E.; Wu, X. Y.; Johnston, M. R. A Novel Trans-Lymphatic Drug Delivery System: Implantable Gelatin Sponge Impregnated with PLGA-Paclitaxel Microspheres. *Biomaterials* **2007,** *28*, 3236–3244.
19. Fang, F.; Gong, C. Y.; Qian, Z. Y.; Zhang, X. N.; Gou, M. L.; You, C.; Zhou, L. X.; Liu, J. G.; Zhang, Y.; Guo, G.; *et al*. Honokiol Nanoparticles in Thermosensitive Hydrogel: Therapeutic Effects on Malignant Pleural Effusion. *ACS Nano* **2009,** *3*, 4080–4088.
20. Dong, Y.; Chin, S. F.; Blanco, E.; Bey, E. A.; Kabbani, W.; Xie, X. J.; Bornmann, W. G.; Boothman, D. A.; Gao, J. M. Intratumoral Delivery of β-Lapachone via Polymer Implants for Prostate Cancer Therapy. *Clin. Cancer Res.* **2009,** *15*, 131–139.
21. Wang, Z. X.; Zhang, Y. W.; Wang, Y. S.; Zhao, J. X.; Wu, C. X. A Way to Prepare Core-Shell Biocompatible Polymeric Nano-Particles from Gelatin and Acrylic Acid. *J. Macromol. Sci., Pure Appl. Chem.* **2006,** *43*, 1779–1786.
22. Hu, Y.; Jiang, X. Q.; Ding, Y.; Chen, Q.; Yang, C. Z. Core-Template-Free Strategy for Preparing Hollow Nanospheres. *Adv. Mater.* **2004,** *16*, 933–937.
23. Li, S. D.; Howell, S. B. CD44-Targeted Microparticles for Delivery of Cisplatin to Peritoneal Matastases. *Mol. Pharmaceutics* **2010,** *7*, 280–290.
24. Campbell, R. B. Tumor Physiology and Delivery of Nanopharmaceuticals. *Anti-cancer Agents Med. Chem.* **2006,** *6*, 503–512.
25. Cao, Y.; Shen, X. C.; Chen, Y.; Guo, J.; Chen, Q.; Jiang, X. Q. pH-Induced Self-Assembly and Capsules of Sodium Alginate. *Biomacromolecules* **2005,** *6*, 2189–2196.
26. Nishiyama, N.; Yokoyama, M.; Aoyagi, T.; Okano, T.; Sakurai, Y.; Kataoka, K. Preparation and Characterization of Self-Assembled Polymer-Metal Complex Micelle from *cis*-Dichlorodiammineplatinum(II) and Poly(ethylene glycol)-Poly(α,β-aspartic acid) Block Copolymer in an Aqueous Medium. *Langmuir* **1999,** *15*, 377–383.
27. Guo, L.; Colby, R. H.; Lusignan, C. P.; Whitesides, T. H. Kinetics of Triple Helix Formation in Semidilute Gelatin Solutions. *Macromolecules* **2003,** *36*, 9999–10008.
28. Zhu, Z. S.; Li, Y.; Li, X. L.; Li, R. T.; Jia, Z. J.; Liu, B. R.; Guo, W. H.; Wu, W.; Jiang, X. Q. Paclitaxel-Loaded Poly(*N*-vinylpyrrolidone)-*b*-Poly(ε-caprolactone) Nanoparticles: Preparation and Antitumor Activity *In Vivo*. *J. Controlled Release* **2010,** *142*, 438–446.
29. Li, S. D.; Huang, L. Pharmacokinetics and Biodistribution of Nanoparticles. *Mol. Pharmaceutics* **2008,** *5*, 496–504.
30. Tseng, C. L.; Wu, S. Y. H.; Wang, W. H.; Peng, C. L.; Lin, F. H.; Lin, C. C.; Young, T. H.; Shieh, M. J. Targeting Efficiency and Biodistribution of Biotinylated-EGF-Conjugated Gelatin Nanoparticles Administered via Aerosol Delivery in Nude Mice with Lung Cancer. *Biomaterials* **2008,** *29*, 3014–3022.
31. Liu, Z.; Cai, W.; He, L.; Nakayama, N.; Chen, K.; Sun, X. M.; Chen, X. Y.; Dai, H. J. *In Vivo* Biodistribution and Highly Efficient Tumour Targeting of Carbon Nanotubes in Mice. *Nat. Nanotechnol.* **2007,** *2*, 47–52.
32. Tang, N.; Du, G. J.; Wang, N.; Liu, C. C.; Hang, H. Y.; Liang, W. Improving Penetration in Tumors with Nanoassemblies of Phospholipids and Doxorubicin. *J. Natl. Cancer Inst.* **2007,** *99*, 1004–1015.
33. Netti, P. A.; Berk, D. A.; Swartz, M. A.; Grodzinsky, A. J.; Jain, R. K. Role of Extracellular Matrix Assembly in Interstitial Transport in Solid Tumors. *Cancer Res.* **2000,** *60*, 2497–2503.
34. Magzoub, M.; Jin, S.; Verkman, A. S. Enhanced Macromolecule Diffusion Deep in Tumors after Enzymatic Digestion of Extracellular Matrix Collagen and Its Associated Proteoglycan Decorin. *FASEB J.* **2008,** *22*, 276–284.
35. Dreher, M. R.; Liu, W. G.; Michelich, C. R.; Dewhirst, M. W.; Yuan, F.; Chilkoti, A. Tumor Vascular Permeability, Accumulation, and Penetration of Macromolecular Drug Carriers. *J. Natl. Cancer Inst.* **2006,** *98*, 335–344.
36. Nishiyama, N.; Kato, Y.; Sugiyama, Y.; Kataoka, K. Cisplatin-Loaded Polymer-Metal Complex Micelle with Time-Modulated Decaying Property as a Novel Drug Delivery System. *Pharm. Res.* **2001,** *18*, 1035–1041.
37. Weinberg, B. D.; Blanc, E.; Gao, J. M. Polymer Implants for Intratumoral Drug Delivery and Cancer Therapy. *J. Pharm. Sci.* **2008,** *97*, 1681–1702.
38. Goodman, T. T.; Olive, P. L.; Pun, S. H. Increased Nanoparticle Penetration in Collagenase-Treated Multicellular Spheroids. *Int. J. Nanomed.* **2007,** *2*, 265–274.
39. Yuan, F.; Leunig, M.; Huang, S. K.; Berk, D. A.; Papahadjopoulos, D.; Jain, R. K. Microvascular Permeability and Interstitial Penetration of Sterically Stabilized (Stealth) Liposomes in a Human Tumor Xenograft. *Cancer Res.* **1994,** *54*, 3352–3356.
40. Menei, P.; Capelle, L.; Guyotat, J.; Fuentes, S.; Assaker, R.; Bataille, B.; Francois, P.; Dorwling-Carter, D.; Paquis, P.; Bauchet, L.; *et al*. Local and Sustained Delivery of 5-Fluorouracil from Biodegradable Microspheres for the Radiosensitization of Malignant Glioma: A Randomized Phase II Trial. *Neurosurgery* **2005,** *56*, 242–247.
41. Cabral, H.; Nishiyama, N.; Okazaki, S.; Koyama, H.; Kataoka, K. Preparation and Biological Properties of Dichloro(1,2-diaminocyclohexane)platinum (II) (DACHPt)-Loaded Polymeric Micelles. *J. Controlled Release* **2005,** *101*, 223–232.